Faculty of Medicine and Life Sciences
School for Life Sciences

Master of Biomedical Sciences

Master's thesis

Purification optimization and tissue localization of a novel biomarker that predict therapy response in rheumatoid arthritis

Sander Sarlée

Thesis presented in fulfillment of the requirements for the degree of Master of Biomedical Sciences, specialization Molecular Mechanisms in Health and Disease

SUPERVISOR :

dr. Sukayna FADLALLAH

Transnational University Limburg is a unique collaboration of two universities in two countries: the University of Hasselt and Maastricht University.

2022
2023

Faculty of Medicine and Life Sciences
School for Life Sciences

Master of Biomedical Sciences

Master's thesis

Purification optimization and tissue localization of a novel biomarker that predict therapy response in rheumatoid arthritis

Sander Sarlée

Thesis presented in fulfillment of the requirements for the degree of Master of Biomedical Sciences, specialization Molecular Mechanisms in Health and Disease

SUPERVISOR :

dr. Sukayna FADLALLAH

Purification optimization and tissue localization of a novel biomarker that predict therapy response in rheumatoid arthritis*

S. Sarlée[1], S. Fadlallah[2] and V. Somers[2,3]

[1]Hasselt University, Campus Diepenbeek, Agoralaan Gebouw D – B-3590 Diepenbeek
[2]Immunology and Infection research group, Biomedical Research Institute, Universiteit Hasselt, Campus Diepenbeek, Agoralaan Gebouw C - B-3590 Diepenbeek
[3]Hasselt University, Hasselt, Belgium

*Running title: *Theranostic antibody biomarker in RA (< 50 characters inc. spaces, italic)*

To whom correspondence should be addressed: Veerle Somers, Tel: +32 (11) 26 92 02; Email: veerle.somers@uhasselt.be

ABSTRACT

Rheumatoid arthritis (RA) is an autoimmune disorder affecting the synovium of joints. One-third of RA patients do not respond to first line treatments leading to prolonged disease activity. Our research group identified 3 novel antibodies (anti-UH-RA.305/318/329) that predict lack of response to first line therapy before treatment initiation. This study aims to optimize the purification of anti-UH-RA.305, and determine its antigenic tissue localization.

To purify anti-UH-RA.305, plasma samples from RA patients were subjected to small column affinity chromatography. The antibody was eluted using 0.1 M glycine-HCl (pH 2.5). Depletion strategies were employed to remove contaminating proteins, and the antibody concentration was measured using phage enzyme-linked immunosorbent assay (ELISA). Anti-UH-RA.305 reactivity was evaluated by competition ELISA where the antibody was incubated with increasing amounts of UH-RA.305 peptide. Immunohistochemistry was performed on synovial knee tissue sections from an RA patient to determine antigenic target expression, with a peptide block for signal validation.

Elution efficiency from the bound column fraction was 54% and 15% from plasma. Competition ELISA confirmed anti-UH-RA.305 reactivity to UH-RA.305 peptide. Immunohistochemistry revealed that the antigenic target of anti-UH-RA.305 was specifically localized in the synovial villus tissue surrounding inflammatory infiltrates. Depletion of the antibody prior to purification enhanced the specificity of the signal detected in immunohistochemistry.

The anti-UH-RA.305 antibody targets fibroblasts in the lining of synovial villi in the joints of RA patients. Targeting these cells may have personalized therapeutic value for the one-third of RA patients experiencing prolonged disease activity due to a lack of treatment response.

INTRODUCTION

Rheumatoid arthritis (RA) affects 18 million people worldwide, with two- to three-fold higher frequency in women than in men (1-3). Patients suffer from joint pain and swelling, physical weakness, and are more susceptible to comorbidities like cardiovascular disease and depression (1, 4-6). RA is a chronic autoimmune disorder, characterized by chronic inflammation of the synovium of joints, which results in cartilage destruction and erosion (3, 4, 7-9). The synovium is a connective tissue encapsulating the joints and is responsible for lubricating the joint surfaces, supplying nutrients to the cartilage and providing structural support (4, 10). Although epithelial cells are absent, the synovium consists of a loose cluster of cells in an extracellular matrix (ECM) together with collagen fibers and other matrix proteins (10). The synovial tissue is composed of two compartments: the intimal lining layer and the sublining layer. The former produces lubricious synovial fluid and comprises two cell types: Type A or macrophage-like synovial cells and Type B or fibroblast like synoviocytes (FLS) (10). Macrophage-like synovial cells are similar to other macrophage populations with phagocytosis as their major function (10). On the other hand, FLS are responsible for producing hyaluronan, an

important component of synovial fluid and ECM and secreting lubricin which is essential for joint lubrication (10, 11). RA-related inflammation transforms the synovium to a tissue marked by intimal lining hyperplasia and infiltrating immunocompetent cells (e.g. $CD4^+$, $CD8^+$ T and B lymphocytes) in the sublining (10, 12). These pathological changes in the synovium can lead to cartilage and bone destruction followed by substantial loss of joint function (4). Fortunately, there are several treatment options available to help manage the symptoms of RA and slow the progression of the disease.

The main therapeutic target for patients is to achieve clinical disease remission with low disease activity (LDA) (4, 13, 14). According to the European League Against Rheumatism (EULAR), the first line of treatment for RA includes using conventional synthetic disease-modifying anti-rheumatic drugs (csDMARDs) (4, 13). Methotrexate (MTX) is the anchor csDMARD in the management of RA (3, 4, 13). The mode of action of MTX is not clearly identified however it is known that MTX acts as a competitive inhibitor of dihydrofolate reductase, an enzyme involved in synthesizing tetrahydrofolate (THF) (3, 15). THF is crucial in DNA and RNA synthesis since it produces purines (3, 15). Accordingly, a disturbed DNA/RNA synthesis causes a reduction in the proliferative capacity of cells (3, 15). Therefore, MTX is believed to alleviate RA symptoms by reducing the proliferation of lymphocytes that contribute to synovial joint inflammation (3, 15). Another possible MOA is the potential of MTX to suppress inflammation by increasing adenosine release from fibroblasts which in turn inhibits the adherence of neutrophils to endothelial cells, thereby decreasing the recruitment of neutrophils to the site of inflammation (3, 15-17). In clinical practice, patients with early RA receive MTX combined with short-term glucocorticoids (GC) (4, 13). The patient is usually evaluated by the rheumatologist to determine if the therapeutic target of remission (or LDA) has been achieved at 6 months post treatment initiation (13). However, approximately one-third of RA patients do not respond to MTX, hence are unable to achieve the therapeutic target (3, 4, 18). Biological DMARDs (bDMARDs) or biologicals, such as tumor necrosis factor (TNF) inhibitors, are usually given as second-line treatment to RA patients who do not respond effectively to first-line therapy (3, 4, 13). Biologicals are designed to target specific molecules involved in the inflammatory process of RA (4, 13). Nonetheless, bDMARDs are expensive and, in Belgium, can only be applied in case of first-line treatment failure, making them a less attractive option for many RA patients (4).

The lack of a prognostic tool for therapeutic response is one of the main reasons that MTX usage is still suboptimal (4, 19). Maciejewski *et al*. determined the serum lipid levels in RA patients, using ultra-performance liquid chromatography mass spectrometry, to investigate if MTX response (by six months) could be predicted. However, the serum lipid profiles were not predictive for therapy response (18). Accordingly, identifying novel biomarkers that can predict treatment response in RA is highly needed. Autoantibodies play an integral role in the pathogenesis of RA (4, 20, 21). Approximately 70-80% of RA patients are positive for autoantibodies (i.e., seropositive), such as rheumatoid factor (RF) and anti-citrullinated protein antibodies (ACPA) (20, 22). RF and ACPA are widely employed in daily practice as diagnostic biomarkers for RA (4, 23). The former is associated with persistent disease, whereas the latter correlates with higher disease activity and a worse disease course (24-27). These autoantibodies can be detected years before the onset of RA (28-30). RF targets the Fc region of immunoglobulin G (IgG) antibodies, which leads to the formation of immune complexes in the synovium (23). These immune complexes can then stimulate immune cells, leading to the release of pro-inflammatory cytokines and perpetuating joint inflammation and injury (23). RF has limited specificity (60-85%) since it can also be found in other rheumatological diseases, such as systemic lupus erythematosus, as well as in healthy donors (20, 22, 31, 32). ACPA comprises a higher diagnostic specificity (85-99%) and is directed to citrullinated proteins, which are proteins that have undergone a post-translational modification called citrullination (22, 23, 32). Citrullination occurs when the amino acid arginine is converted into citrulline by an enzyme called peptidyl arginine deiminase (23). Sokolove *et al*. demonstrated that ACPA can form complexes with citrullinated fibrinogen in the RA
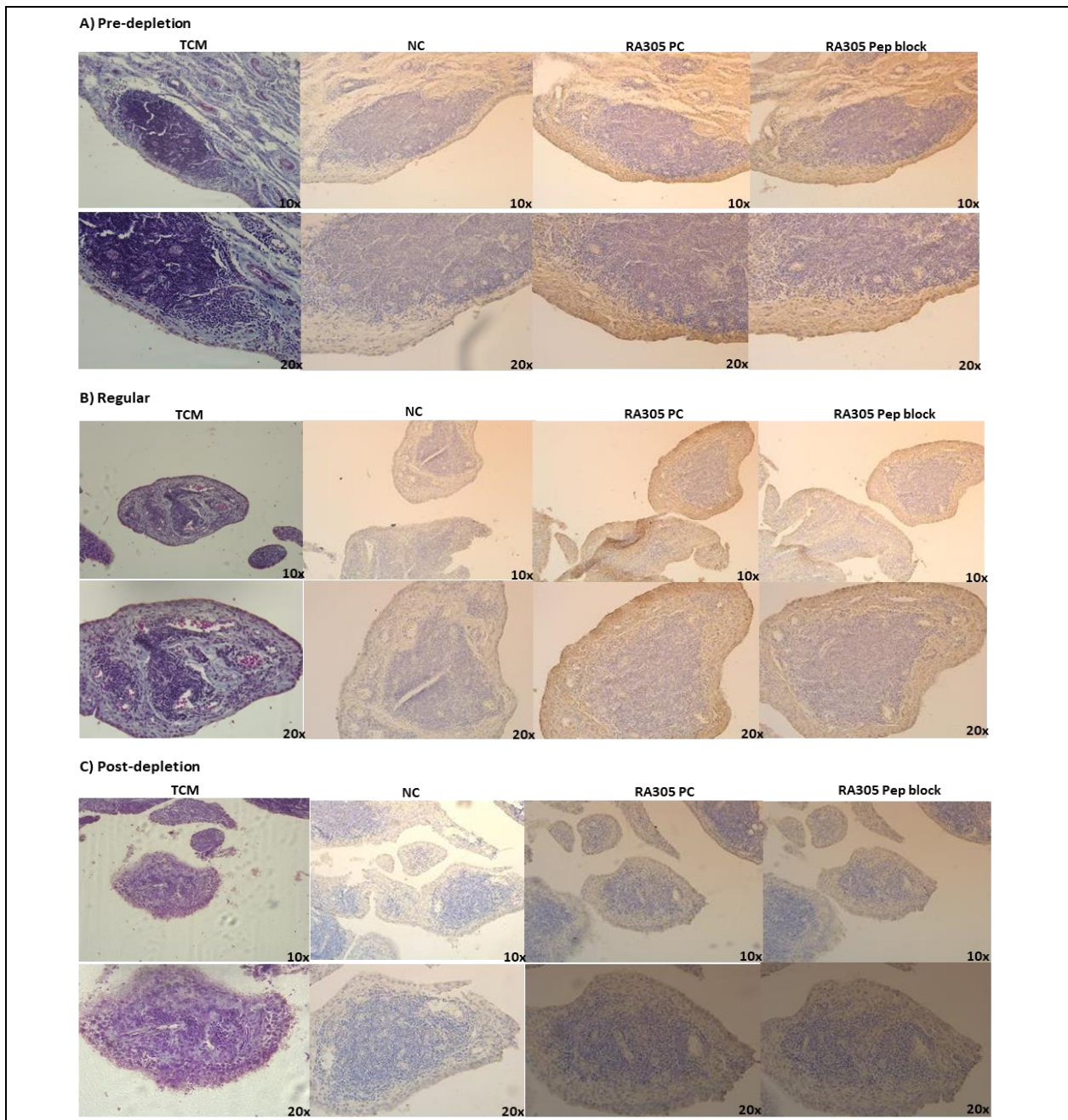
2

Fig.1 – Synovial tissue expression of the *in vivo* antigenic target of pre-depleted, regular and post-depleted purified anti-UH-RA.305. (A-C) Representative staining of synovial knee tissue sections from one RA patient. NC, i.e. tissue incubated with 1xPBS, showed no staining. (A&B) RA305 PC, i.e. tissue incubated with pre-depleted and regular purified anti-UH-RA.305, showed staining (brown) in the lining of synovial villus surrounding inflammatory infiltrates. RA305 pep block, i.e. tissue incubated with anti-UH-RA305 and 4 mg/ml of UH-RA.305 peptide, showed reduced staining in the synovial lining. The peptide block showed less staining in the pre-depleted purified anti-UH-RA.305, indicating higher antigen specificity. (C) The positive control and RA305 peptide block is similar to the negative control, indicating that depletion of anti-UH-RA.305 antibody following its purification displays the least antigen specificity. Staining was performed with DAB (brown) and haematoxylin mayer counterstaining (blue). TCM: Trichrome Masson staining, NC: Negative Control; PC: Positive Control; Pep: peptide

synovium *in vitro*, which stimulates macrophages to produce TNF-α, thereby promoting joint inflammation (33). RF can amplify this inflammatory response by stimulating TNF-α production and the release of other pro-inflammatory cytokines (34). Kuhn *et al.* evaluated the role of ACPA *in vivo* by using the collagen-induced arthritis (CIA) mice model, an

animal model that recapitulates RA (35). Here, it was demonstrated that autoantibodies against citrullinated proteins such as fibrinogen and collagen substantially enhance joint tissue injury (35). Additionally, ACPA has been shown *in vitro* and *in vivo* to stimulate bone loss by binding to citrullinated vimentin on osteoclast surfaces leading to the induction of osteoclastogenesis and bone resorption (36, 37). Hence, these autoantibodies play an active role in RA disease pathogenesis.

Interestingly, besides the diagnostic characteristic of RF and ACPA, these autoantibodies have also been investigated in predicting therapy response. For example, a number of studies suggest that RF and ACPA seropositivity predicts an effective response to rituximab, a monoclonal antibody that selectively depletes B cells (38-41). Regarding the clinical response to TNF inhibitors, the presence of RF and ACPA was found to be not predictive (42). Additionally, numerous studies, including early and established RA patient populations, have shown that the presence of RF does not predict response to MTX (43-46). However, a study by Wessels *et al.* and Gossec *et al.* demonstrated that RF seropositive RA patients tended to display a worse response to MTX and a lower remission rate, respectively (47, 48). Conversely, RF seronegativity was associated with disease remission over a four-year period (49). Although, it should be noted that these findings were probably directly related to the role of RF as a marker of persistent and severe disease rather than therapy effectiveness. Likewise, ACPA was not shown to influence MTX effectiveness (45, 47). Some contradicting studies reported a lower response to treatment in ACPA-positive patients (50, 51). This could possibly be due to the higher disease activity that is associated with ACPA.

As previously mentioned, identifying novel biomarkers that are able to predict response to first-line DMARDs is highly needed. A study found that higher levels of naïve cluster of differentiation (CD)4-positive T cells were associated with disease remission in response to MTX, compared to healthy controls (52). Additionally, the level of CD39 on regulatory T cells (Tregs) was found to predict MTX treatment response (53). Patients who did not reach remission expressed less CD39 on Tregs than healthy controls (53). These immunological biomarkers seem to have predictive value, but a serological marker would be more convenient for clinical testing.

Our research group identified, using cDNA phage display, antibodies to three Hasselt University (UH) peptides, UH-RA.305, UH-RA.318 and UH-RA.329 that can predict lack of treatment response before treatment initiation (54). In the study, a total of 219 early RA patients were included from the Care in early RA (CareRA) trial (54). The CareRA trial is a trial that spanned a duration of 2 years to evaluate and compare the efficacy of various treatment regimens for patients diagnosed with early RA (54, 55). Before initiation of first-line csDMARD treatments, baseline serum samples were collected from the 219 RA participants (54). Additionally, messenger RNA was extracted from hip and knee synovial tissue samples of 4 RA patients and converted into complementary DNA (cDNA) (54). The cDNA was then inserted into a phage vector (M13 filamentous phage) that displays the cDNA-encoded proteins on its surface. Accordingly, two cDNA phage display libraries were constructed. These libraries consisted of a wide range of phage particles screened against antibodies in baseline serum pools (n=20) which were derived from RA patients that did not reach remission after 16 weeks of first-line therapy (54). This screening identified increased antibody reactivity, in remission-negative serum pools, for six UH-RA antigens. Validation in 179 additional RA serum samples, from participants of the CareRA trial, and in 86 age- and gender-matched healthy controls (IMMHC), revealed immunoreactivity against three antigens that showed the best predictive value for remission: anti-UH-RA.305/318/329 (54).

However, the biological role of these antibodies is currently unknown. The aim of the present study is to optimize the purification for two of the three antibodies (anti-UH-RA.305/318) from plasma of RA patients. Purification conditions have already been optimized for anti-UH-RA.329. Furthermore, the synovial tissue expression of the antigenic target of anti-UH-RA.305 will be investigated. Overall, understanding the biological rationale of anti-UH-RA.305/318/329 in predicting therapy response contributes to the concept of personalized medicine and can potentially lead to the identification of new therapeutic targets to improve the management of RA.

EXPERIMENTAL PROCEDURES
Optimizing immuno-affinity purification of anti-UH-RA.305/318 and storage of anti-UH-

RA.305 – Antibody purification was conducted by coupling the synthetic biotinylated UH-RA.305/318 peptide (GL Biochem, Shanghai, China) to Pierce™ Spin Columns (Thermo Fisher Scientific, Waltham, United States). The UH-RA.305/318 coupled column was incubated for 1 hour at 4°C with plasma known by phage Enzyme Linked Immunosorbent Assay (ELISA) to comprise high levels of anti-UH-RA.305/318 antibodies. Different strategies of depletion (i.e. removing contaminating proteins from the plasma) were implemented by coupling a control peptide to the column before or after purification of the antibody. The coupling efficiency of control and UH-RA.305/318 peptide was measured with Nanodrop 2000 Spectrophotometry (Thermo Fisher Scientific). The column was then centrifuged at 500 g for 1 minute, to collect the flowthrough fraction, after which it was washed three times in 1x PBS. Anti-UH-RA.305 was eluted for 2 minutes at room temperature using 0.1 M glycine-hydrochloride (HCl) as elution buffer (pH 2.5). This was followed by immediate neutralization with 1 M Tris-HCL (pH 9). Regarding the purification of anti-UH-RA.318, 0.1 M glycine-HCl leads to antibody reactivity loss. Consequently, different elution buffers were tested to optimize the antibody reactivity following elution. These buffers include 4.5 M magnesium chloride ($MgCl_2$); 3.6 M $MgCl_2$; 3.5 M potassium chloride (KCl); 4.5 M $MgCl_2$ + 25% ethylene glycol; 4.5 M $MgCl_2$ + 25% ethylene glycol + 0.075 M Hepes + sodium hydroxide (NaOH) (pH 7.2), and 0.1 M glycine-NaOH (pH 10). The column was then centrifuged at 500 g for 1 minute to collect the eluted antibody fractions. The elution efficiency of anti-UH-RA.305/318 from the bound column fraction and total plasma was evaluated by phage ELISA.

Additionally, the storage of the eluted anti-UH-RA.305 antibody was optimized. The antibody was stored at 4°C and -20°C. To enable freezing at -20°C, the purified antibody solution was mixed with equal amounts of 100% glycerol (50% glycerol/50% antibody). The concentration of antibody, displayed in AU/µl, was measured over time with phage ELISA.

Phage Enzyme Linked Immunosorbent Assay –Following purification, the level of antibody reactivity was measured by phage ELISA. Half area 96-well Microlon high-binding microplates (Greiner Bio-One, Frickenhausen, Germany) were coated overnight at 4°C with 0.5 µg/ml anti-M13 mouse monoclonal antibody (Sino Biological, Bejing, China) diluted in coating buffer. Plates were washed once short, twice for 3 minutes in 0.1% PBS-Tween (PBS-T) and once for 3 minutes in 1x PBS. Plates were then blocked with 5% PBS-Marvel (PBS-M) for 2 hours shaking at 37°C. After blocking, plates were washed 1xshort and 2x3 min with 0.1% PBS-T and 1x3 min with PBS. Plates were incubated with 7 x 10^{11} colony forming units/ml of phage particles displaying the corresponding antigen (specific phage) and phage particles without antigen (empty phage) for 1 hour at 37°C and 30 minutes shaking at room temperature. Plates were washed 1xshort and 2x3 min with 0.1% PBS-T and 1x3 min with PBS. The phage particles were incubated with plasma samples for 1 hour at 37°C and 30 minutes shaking at room temperature. Consequently, plates were washed 1xshort and 2x3 min with 0.1% PBS-T and 1x3 min with PBS. Plates were then incubated with goat anti-human biotinylated IgG antibody (Sanbio, Uden, The Netherlands) conjugated to streptavidin poly-horse radish peroxidase (HRP) (Thermo Fisher Scientific) for 1 hour at room temperature. This was followed by color development with 1-Step™ Ultra TMB-ELISA (Thermo Fisher Scientific). The reaction was stopped by addition of 1.8 N sulfuric acid and color development was read at 450 nm by the CLARIOstar®Plus plate reader (BMG LABTECH, Ortenberg, Germany). A ratio of OD (UH-RA.305 phage)/OD(empty phage) of more than 1.5 was implemented as cut-off for an antibody-positive signal. Samples were tested in duplicate within each phage ELISA experiment. A sample known to contain anti-UH-RA.305 antibody reactivity was included as positive control. A series of dilution of that sample was used to plot a standard curve. Based on the standard curve, the eluted antibody concentration, in arbitrary units (AU), was determined. Testing different possible positive samples in order to optimize the standard curve was necessary.

Competition ELISA – To validate that the UH-RA.305 phage displayed peptide is the specific target of the anti-UH-RA.305 antibody and to ensure specificity of staining, a competition ELISA was conducted. The purified antibody sample was pre-incubated with increasing concentrations (ranging from 0 to 10 µg/ml) of UH-RA.305 peptide and control peptide, for one hour shaking at room temperature. Following the pre-incubation, the samples were used in a standard phage ELISA as previously described. Pre-incubation with

increasing concentrations of control peptide was used as a negative control.

Immunohistochemical analysis of RA synovial tissue – To identify the tissue expression of the antigenic target of anti-UH-RA.305, immunohistochemistry was performed on formalin-fixed, paraffin-embedded knee synovial tissue sections from human RA patients.

Sections were deparaffinized twice for a period of 5 minutes each in xylene followed by 2 minutes rehydration in a series of decreasing ethanol concentrations (100% → 70%) and distilled water. Sections were washed once for 5 minutes shaking with distilled water and antigen retrieval was conducted using heated citrate buffer at 60°C for 1.5 hours in a heat bath. Sections were washed in 1x PBS three times for 5 minutes for each wash. This was followed by blocking with undiluted DAKO Protein block serum free (Dako, Glostrup, Denmark) for 30min at room temperature. Anti-UH-RA antibody (1:2 in 1x PBS) was incubated overnight at 4°C. Slides were washed in 1x PBS three times, 3 minutes for each wash. Endogenous peroxidase activity was blocked by incubation in 0.3% (v/v) hydrogen peroxide in methanol for 10 minutes. Slides were then washed in 1x PBS three times for 3 minutes for each wash followed by incubation with streptavidin poly HRP (1:500 in 1x PBS) at room temperature for 30 minutes. Slides were washed in 1x PBS three times for 3 minutes for each wash followed by staining with 3,3' diaminobenzidine (DAB) (Sigma-Aldrich, Missouri, United States) for 10 minutes at room temperature. Sections were washed three times in distilled water, 3 minutes for each wash followed by counterstaining with hematoxylin for 1 minute. Sections were rinsed under tap water for 10 minutes and dehydrated for 2 minutes in a series of increasing ethanol concentrations (70% → 100%). Sections were immersed in xylene twice for a period of 5 minutes for each immersion and coverslipped with DPX mounting medium.

Analysis of the stained sections was performed with a Leica DM2000 Dual Viewing microscope. In addition, the immunohistochemistry results were validated with two pathologists.

Optimizing immunohistochemical staining of vimentin and cluster of differentiation 68 in RA synovial tissue – To determine potential colocalization of the anti-UH-RA.305 antibody and cells in the synovial lining, DAB staining was optimized on formalin-fixed, paraffin-embedded knee synovial tissue sections for vimentin and cluster of differentiation 68 (CD68). Staining was performed as previously described, while some adaptations were implemented. Sections were blocked with rabbit serum for one hour at room temperature. Overnight incubation at 4°C was performed with Monoclonal Mouse Anti-Vimentin primary antibody (Dako) and Monoclonal Mouse Anti-Human CD68 primary antibody (Dako). Polyclonal Rabbit Anti-Mouse IgG/HRP (Dako) was used as secondary antibody and incubated at room temperature for 30 minutes. Various primary antibody dilutions (1:50, 1:100, 1:200 in 1xPBS) and secondary antibody dilutions (1:200 to 1:400 in 1xPBS) were tested to identify the optimal vimentin and CD68 staining conditions.

Trichroom Masson staining – Sections were deparaffinized and rehydrated as previously described. Subsequently, sections were immersed in hematoxylin for 7 minutes, rinsed under running tap water for 20 minutes, incubated in ponceau/fuchsine solution for 5 minutes followed by 2 minutes in distilled water. Next, the sections were treated with 5% phosphomolybdic acid (5 minutes) and distilled water (2 minutes), stained with aniline blue solution (5 minutes), rinsed with distilled water (2 minutes), treated with 1% phosphomolybdic acid (5 minutes) and distilled water (1 minute), immersed in 1% acetic acid (2 minutes) and distilled water (1 minute). Dehydration was achieved by dipping the sections in 70%, 80%, and 95% ethanol, followed by 2 minutes in 100% ethanol. Finally, the sections were immersed in xylene (2x5 minutes) and coverslipped with DPX mounting medium.

RESULTS

Optimizing immuno-affinity purification of anti-UH-RA.318 – The challenge in purifying anti-UH-RA.318 was the inability to elute the antibody effectively. For purifying anti-UH-RA.305/329, 0.1 M glycine-HCL, an acidic elution buffer (pH 2.5), worked optimally. However, glycine-HCL led to reactivity loss of the anti-UH-RA.318 antibody. In addition to 4.5 M and 3.6 M $MgCl_2$, 3.5 M KCl, 0.1 M glycine-NaOH (pH 10), 4.5 M $MgCl_2$ with 25% ethylene glycol, 4.5 M $MgCl_2$ with 25% ethylene glycol together with 0.075 M HEPES and NaOH (pH 7.2) were tested. A standard curve was included to calculate the arbitrary units (AU) and percentages of bound and purified (elution) fraction.

Overall, the UH-RA.318 peptide coupling efficiency was 64%. Regarding the elution

efficiency from the bound column fraction and total plasma, purification was still suboptimal for the six elution buffers (data not shown).
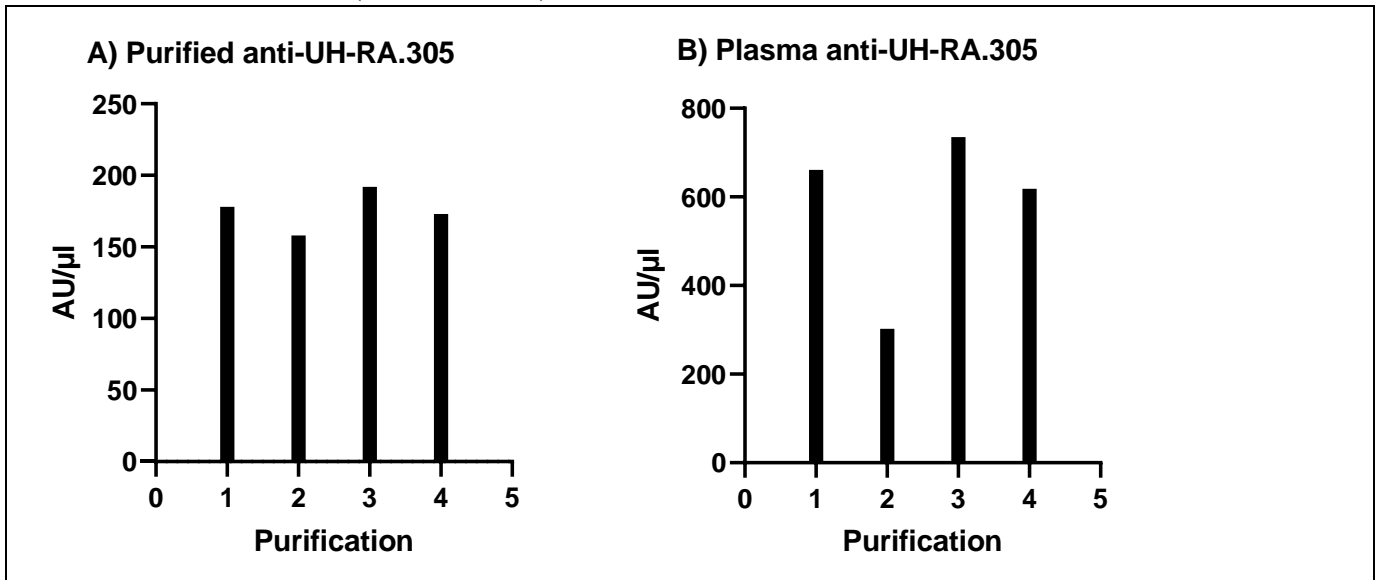

Fig.2 – The elution stability of pre-depleted purified and plasma anti-UH-RA.305. Four independent purifications were conducted to evaluate the anti-UH-RA.305 antibody concentration. The eluted antibody concentration is expressed in AU/µl, measured using phage ELISA. On the y-axis, the AU/µl is displayed whereas the x-axis depicts the corresponding purification round (n=4). (A) Purification 1: 178 AU/µl, Purification 2: 158 AU/µl, Purification 3: 192 AU/µl and Purification 4: 173 AU/µl. Overall, the antibody concentration remained relatively stable with an average of 175 AU/µl. (B) The average concentration of anti-UH-RA.305 antibody in plasma was 579 AU/µl. The absorbance is measured at 450 nm. AU: Absorbance Units
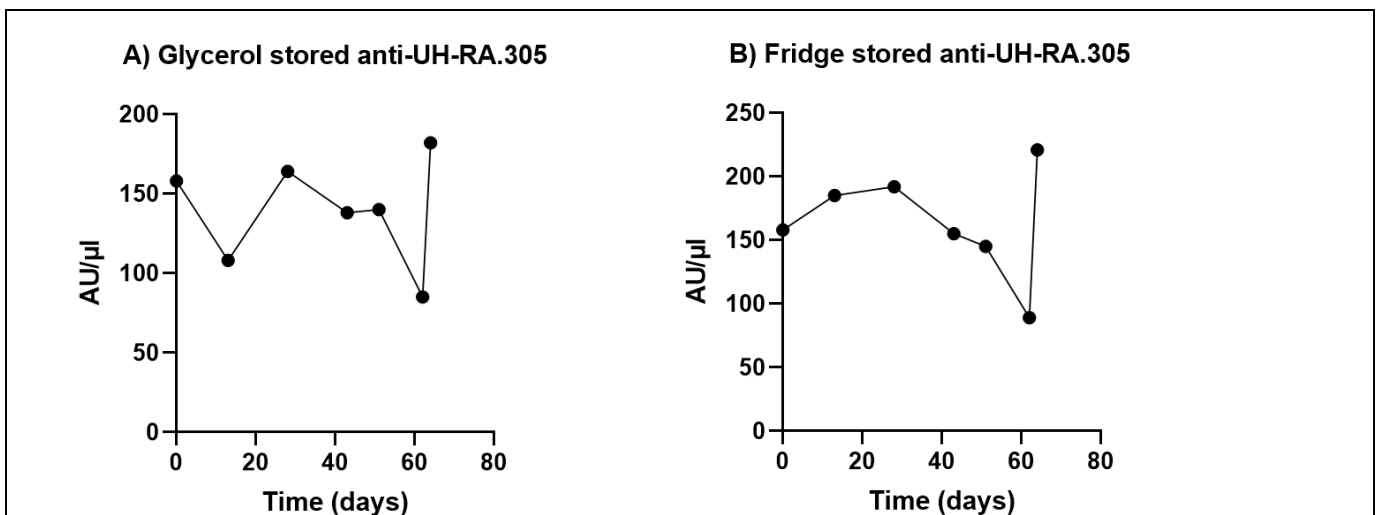

Fig.3 – Optimizing the storage condition of pre-depleted purified anti-UH-RA.305. (A) The pre-depleted purified anti-UH-RA.305 antibody was mixed with equal amounts of glycerol solution (i.e. 50% Antibody/50% Glycerol) and stored at -20°C. (B) The pre-depleted purified anti-UH-RA.305 antibody was stored at 4°C in the fridge. On the y-axis, the AU/µl is displayed whereas the x-axis depicts the time in days. The AU/µl is measured at each timepoint over the 9 weeks period using phage ELISA. (A&B) The antibody concentration at baseline (day 0) was 158 AU/µl. Hereafter, the AU/µl values remained relatively constant within the range of 136 AU/µl and 165 AU/µl for glycerol and fridge storage conditions, respectively. The absorbance is measured at 450 nm. AU: Absorbance Units

Optimizing immuno-affinity purification of anti-UH-RA.305 – To optimize the immuno-affinity purification of anti-UH-RA.305, the crude RA305 antibody plasma was depleted before and after purification. The average control and UH-RA.305 peptide coupling efficiency was 58% and 69%, respectively. Furthermore, based on phage ELISA, the eluted antibody was reactive against the phage displaying UH-RA.305 peptide in both depletion conditions as the ratio of OD (UH-RA.305 phage) to OD (empty phage) was above the cut-off value of 1.5. The sample that was initially used to plot a standard curve was IMMHCp0261-t1. However, it was not possible to calculate the elution efficiency as the standard curve displayed high background antibody

positivity (i.e. ratio), were selected from the CareRA trial. The sample with the highest ratio, IMMHCp082-t1, was used as the standard curve in the following anti-UH-RA.305 purifications.

Anti-UH-RA.305 targets specifically synovial villi and pre-depletion shows greatest antigen specificity – To gain insight into the tissue expression of the antigenic target of pre-depleted, regular purification and post-depleted anti-UH-RA.305, immunohistochemical analysis was carried out on synovial knee tissue sections from one RA patient (Fig.1A-C). Sections were stained using DAB (brown) and counterstained with haematoxylin mayer (blue). In addition, the tissue was counterstained with TCM for visualization of tissue integrity and cellular morphology.
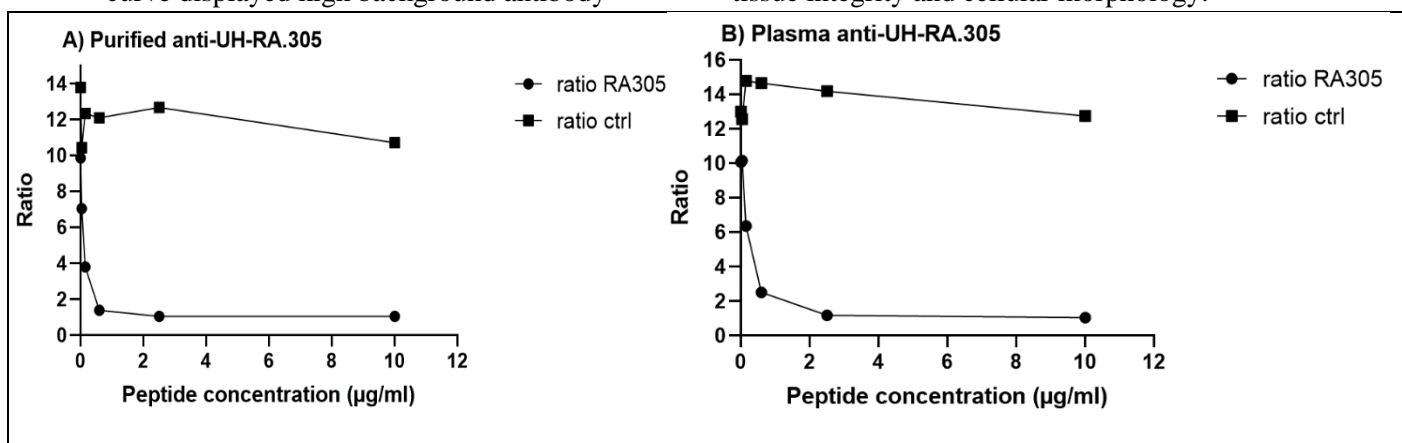

Fig.4 – **Competition ELISA confirms reactivity of anti-UH-RA.305 against the UH-RA.305 peptide.** In a competition ELISA, the sample is pre-incubated with increasing amounts of synthetic peptide. If the peptide effectively competes with the phage displayed peptide for antibody binding, there will be a decrease in OD signals with increasing peptide concentration. On the y-axis, the peptide (RA305 and control) concentration in µg/ml is displayed whereas the x-axis depicts the ratio. The ratio is defined as the average OD of tested phage (i.e. UH-RA-305 phage) divided by the average OD of empty phage. (A&B) As a negative control, samples are pre-incubated with increasing amounts of irrelevant control peptide. The ratio does not decrease with increasing control peptide concentration as no competition exist with the antibody. (A) The ratio of anti-UH-RA.305 antibody tends from an antibody-positive to an antibody-negative ratio with increasing UH-RA.305 peptide concentration. (B) As a positive control, the anti-UH-RA.305 plasma was included. The absorbance is measured at 450 nm. Ctrl: control

reactivity (i.e. high OD(empty phage)). Hence, optimizing the standard curve was of utmost importance. First, a new aliquot of the standard curve was tested. Second, different batches of UH-RA.305 and empty phage were incorporated. Additionally, HRP-labeled goat anti-human IgG was included as a detection method and compared with the currently used method (i.e. goat anti-human biotinylated IgG antibody conjugated to streptavidin poly-HRP). Nonetheless, these adaptations did not resolve the high background reactivity. Accordingly, eight novel healthy control samples, based on antibody-

Tissue sections were incubated with 1x PBS as negative control (Fig.1A-C). The negative control showed no staining, confirming the absence of nonspecific binding (Fig.1A-C). Interestingly, pre-depleted and normal purified anti-UH-RA.305 antibody target specifically synovial villus tissue surrounding inflammatory infiltrates (Fig.1A&B). Antigen specificity was evaluated by incubating the anti-UH-RA.305 antibody with 4 mg/ml UH-RA.305 peptide (Fig.1A-C). The antigen specificity was less pronounced in the normal purified anti-UH-RA.305 as compared to pre-depletion (Fig.1A&B). Additionally, post-depletion
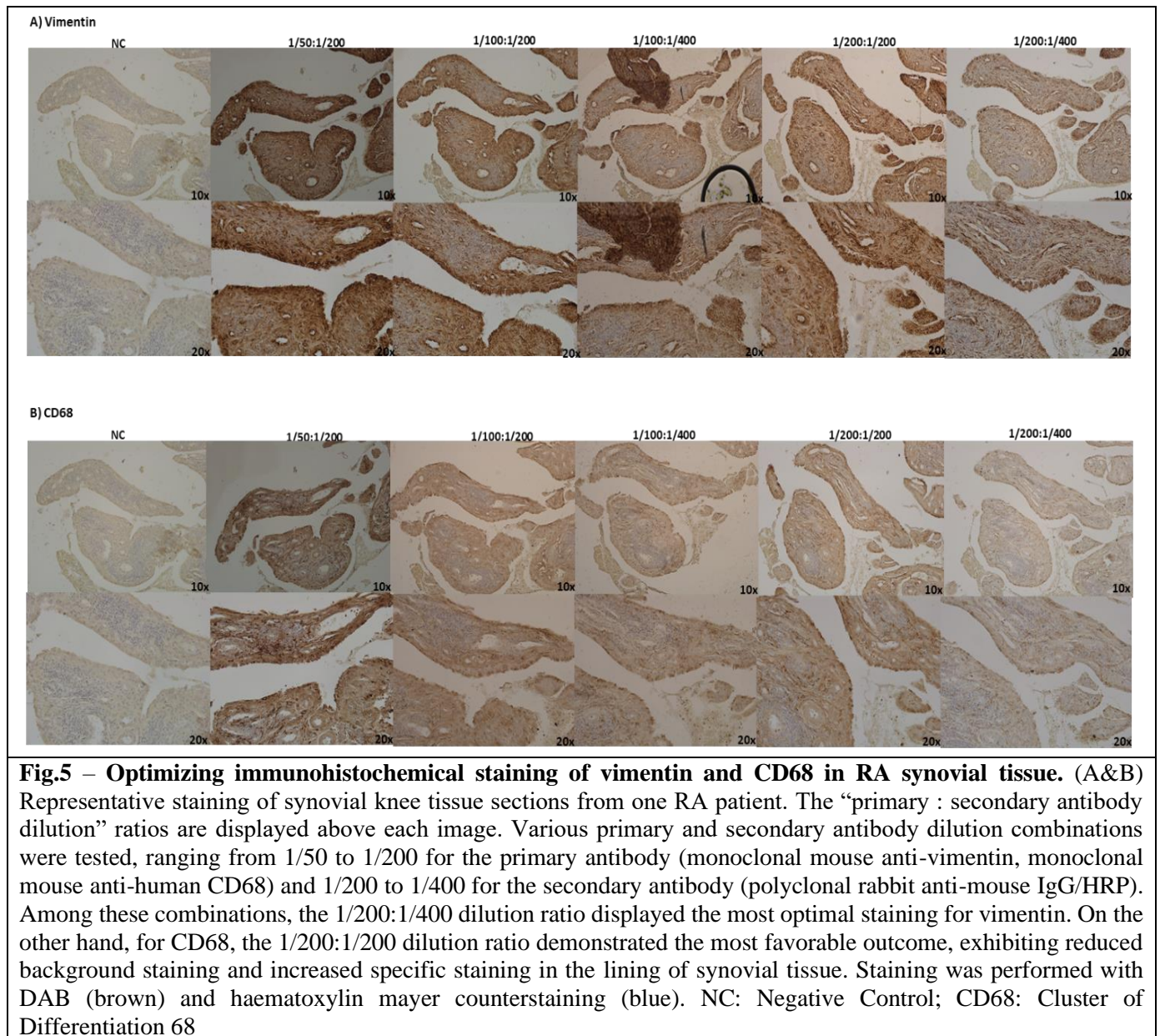
Fig.5 – Optimizing immunohistochemical staining of vimentin and CD68 in RA synovial tissue. (A&B) Representative staining of synovial knee tissue sections from one RA patient. The "primary : secondary antibody dilution" ratios are displayed above each image. Various primary and secondary antibody dilution combinations were tested, ranging from 1/50 to 1/200 for the primary antibody (monoclonal mouse anti-vimentin, monoclonal mouse anti-human CD68) and 1/200 to 1/400 for the secondary antibody (polyclonal rabbit anti-mouse IgG/HRP). Among these combinations, the 1/200:1/400 dilution ratio displayed the most optimal staining for vimentin. On the other hand, for CD68, the 1/200:1/200 dilution ratio demonstrated the most favorable outcome, exhibiting reduced background staining and increased specific staining in the lining of synovial tissue. Staining was performed with DAB (brown) and haematoxylin mayer counterstaining (blue). NC: Negative Control; CD68: Cluster of Differentiation 68

displayed the least antigen specificity as the positive control and RA305 peptide block were similar to the negative control (Fig.1C). Overall, the antigenic target of anti-UH.RA.305 is expressed in the synovial villi of the joint of RA patients. Furthermore, the depletion of anti-UH-RA.305 antibody prior to its purification yielded the greatest antigen specificity.

Optimizing pre-depletion immuno-affinity purification of anti-UH-RA.305 – As evidenced by immunohistochemical analysis, pre-depletion showed superior antigen specificity as compared to regular and post-depleted anti-UH-RA.305. Accordingly, anti-UH-RA.305 was pre-depleted in each purification. The control and UH-RA.305 peptide coupling efficiency varied from 58% to 69% and 59% to 69.7%, respectively. The average elution efficiency from the bound column

fraction and total plasma was 54% and 15%, respectively. Besides optimizing the antibody purification, the elution stability was taken into account (Fig.2). Upon conducting four independent purifications, the antibody concentration was assessed using phage ELISA, reported as AU/µl. The eluted anti-UH-RA.305 antibody concentration ranged from 158 AU/µl to 192 AU/µl, with an average of 175 AU/µl, indicating that the elution remained relatively stable (Fig.2A). Furthermore, the average concentration of anti-UH-RA.305 in plasma comprised 579 AU/µl (Fig.2B).

Additionally, the purified antibody was stored at 4°C and -20°C (i.e. 50% antibody/50% glycerol) over a 9 weeks period, to optimize the storage condition (Fig.3). Each data point represents the AU/µl measured on the
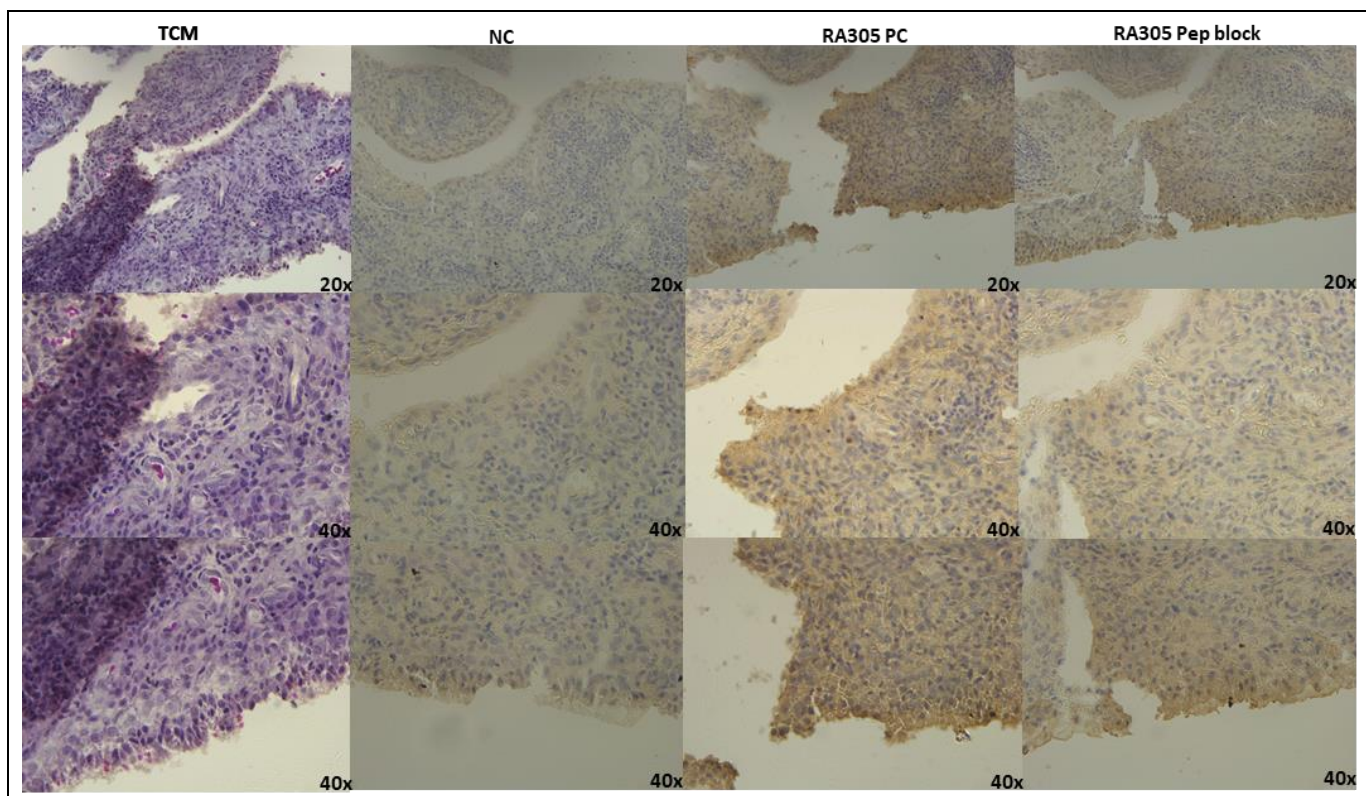
Fig.6 – **The anti-UH-RA.305 antibody specifically targets fibroblasts in the synovial lining.** Representative staining of synovial knee tissue sections from one RA patient. NC, i.e. tissue incubated with 1xPBS, showed no staining. RA305 PC, i.e. tissue incubated with pre-depleted purified anti-UH-RA.305, specifically targets fibroblasts in the lining of synovial villus surrounding inflammatory infiltrates. RA305 pep block, i.e. tissue incubated with anti-UH-RA305 and 4 mg/ml of UH-RA.305 peptide, showed reduced staining in the synovial lining. Staining was performed with DAB (brown) and haematoxylin mayer counterstaining (blue). TCM: Trichroom Masson; NC: Negative Control; PC: Positive Control; Pep: Peptide

corresponding timepoint using phage ELISA. At baseline (day 0), 158 AU/µl of anti-UH-RA.305 was eluted from total plasma. Hereafter, the AU/µl values remained relatively constant within the range of 136 AU/µl and 165 AU/µl for glycerol and fridge storage conditions, respectively (Fig.3).

Anti-UH-RA.305 is reactive against the UH-RA.305 peptide displayed on the UH-RA-305 phage – To validate whether the pre-depleted purified (elution) fraction of anti-UH-RA.305 is reactive against the UH-RA.305 peptide, a competition ELISA was carried out (Fig.4). The plasma was included as positive control (Fig. 4B). On the one hand, the antibody-positive signal was retained across the range of control peptide concentration as the ratio was above 1.5 (Fig.4). On the other hand, the antibody-positivity decreased with increasing UH-RA.305 peptide concentration (0 µg/ml to 10µg/ml) (Fig.4). Specifically, 0.6 µg/ml of UH-RA.305 peptide was needed to compete with the phage displayed peptide for pre-depleted anti-UH-RA.305 antibody binding. The positive control (i.e.,

plasma known to comprise high levels of anti-UH-RA.305) displayed a similar competition trend, confirming the reliability of the assay (Fig.4B). Here, 2.5 µg/ml of UH-RA.305 peptide was needed to block antibody binding.

Optimizing immunohistochemical staining of vimentin and CD68 in RA synovial tissue to investigate potential colocalization of the anti-UH-RA.305 antibody – As previously demonstrated, the anti-UH-RA.305 antibody specifically targets the lining of the synovial villi in the joint of RA patients (Fig.1). To determine potential colocalization of the antibody and synoviocytes in the synovial lining, DAB staining was optimized for vimentin and CD68 (Fig.5). Various combinations of primary and secondary antibody dilutions were tested to identify the optimal condition for vimentin and CD68 staining. Among the tested antibody dilution combinations, the 1/50:1/200 dilution ratio resulted in the highest background staining for both vimentin and CD68 (Fig.5A&B). This
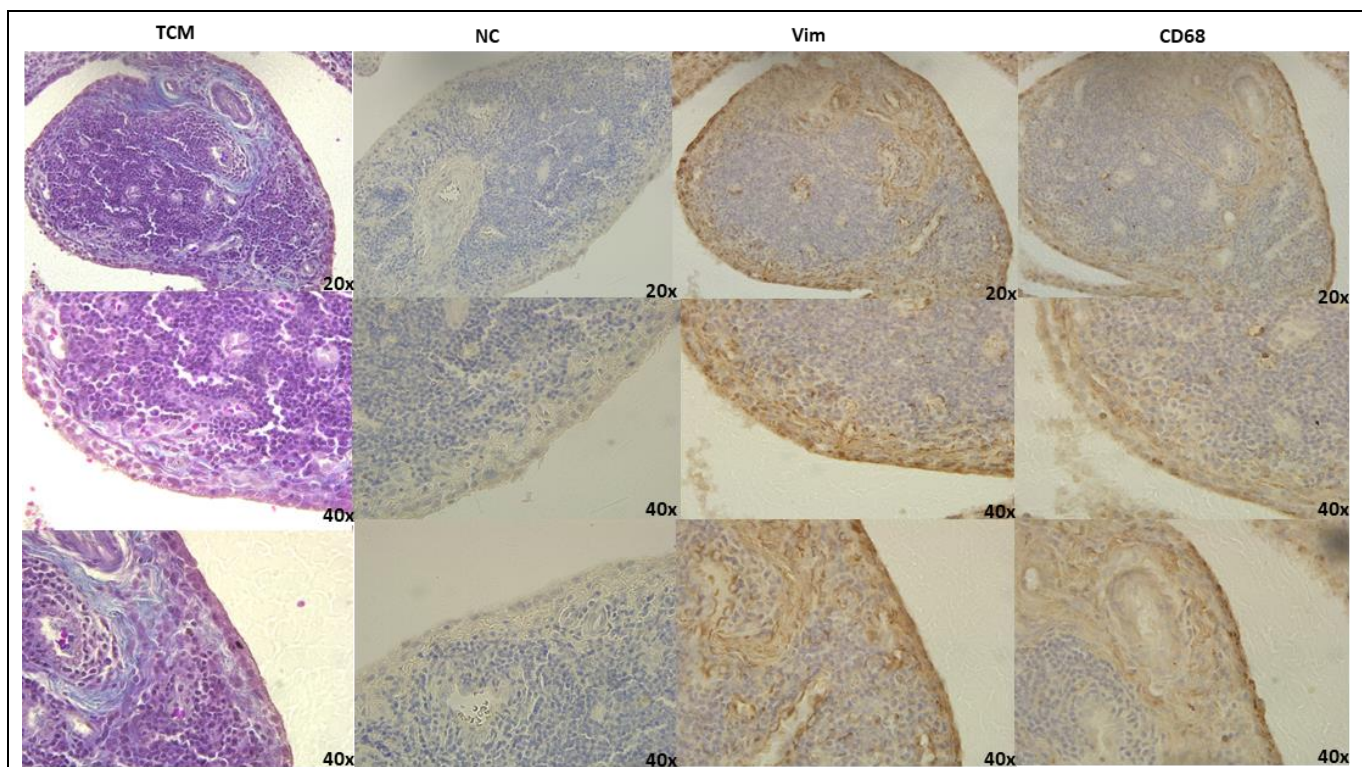
Fig.7 – V**imentin and CD68 specifically targets the synovial lining.** Representative staining of synovial knee tissue sections from one RA patient. NC, i.e. tissue incubated with 1xPBS, showed no staining. Vimentin (1/200:1/400 dilution ratio) and CD68 (1/200:1/200 dilution ratio) stains the lining of synovial villus. Staining was performed with DAB (brown) and haematoxylin mayer counterstaining (blue). TCM: Trichroom Masson; NC: Negative Control; Vim: Vimentin; CD68: Cluster of Differentiation 68

combination displayed increased non-specific binding, leading to elevated background signal and reduced specificity of staining for the target proteins. The subsequent adjustment of the dilution ratios to 1/200:1/400 for vimentin and 1/200:1/200 for CD68 successfully mitigated the background staining while maintaining specific staining signals in the RA synovial tissue (Fig.5).

Anti-UH-RA.305 targets fibroblasts in the synovial lining – The establishment of optimized staining conditions for vimentin and CD68 in RA synovial tissue led to further investigation regarding the localization of the anti-UH-RA.305 antibody staining (Fig.6-8).

The negative control showed no detectable staining in the synovial tissue, demonstrating the absence of non-specific binding of the antibody (Fig.6-8). As previously demonstrated, the anti-UH-RA.305 antibody displayed specific staining in the lining of synovial villi (Fig.1, Fig.6&8). Notably, vimentin and CD68 demonstrated a similar region of staining (i.e. the synovial lining), indicating a potential colocalization of the antibody with vimentin and/or CD68 within the synovial lining of an RA patient (Fig.7&8). After thorough analysis of the staining with renowned

pathologists, the anti-UH-RA.305 antibody specifically targets fibroblasts in the synovial lining.

DISCUSSION

To gain further insight into the biological role of anti-UH-RA.305, we focused on optimizing the purification of anti-UH-RA.305 and characterizing the antigenic target tissue expression of anti-UH-RA.305 in knee synovial tissue samples of RA patients.

Optimizing immuno-affinity purification of anti-UH-RA.305 and alternative purification methods – Immuno-affinity purification of anti-UH-RA.305 demonstrated an overall elution efficiency of 54% from the bound column fraction and 15% from total plasma. In addition to immuno-affinity chromatography, different purification approaches can be employed to isolate antibodies: protein A/G affinity chromatography, ion exchange chromatography (IEX), size exclusion chromatography (SEC) and magnetic bead-based purification (56). Protein A/G affinity chromatography is considered to be the gold standard for antibody purification (57). Both Protein A and Protein G, bacterial proteins,

possess a strong affinity for the Fc region of IgG antibodies from various species such as human, mouse, rat, and rabbit, ensuring efficient and selective binding (58). IEX is another widely used technique for antibody purification wherein antibodies can be separated from other plasma proteins based on their net charge (56). Elution is typically achieved by increasing salt concentration in a gradient elution process (56, 59). SEC, or gel filtration chromatography, separates proteins by size and molecular weight and can be used to further refine the antibody sample (56, 59). Magnetic bead-based purification utilizes magnetic beads functionalized with a specific ligand to capture the target antibody, eliminating the need for centrifugation (60). In this regard, magnetic bead-based purification follows the same concept as immuno-affinity chromatography, utilizing a ligand-antibody interaction, however magnetic beads may incur slightly higher costs, and optimizing the protocol for anti-UH-RA.305 will be time-consuming. Protein A/G purification isolates IgG antibodies but does not specifically purify antibodies targeted against a particular ligand. IEX and SEC rely on specific antibody characteristics for purification. However, the anti-UH-RA.305 antibody profile is currently unknown, which presents a challenge in utilizing IEX and SEC purification techniques. In the future, we aim to characterize the anti-UH-RA.305 antibody by employing mass spectrometry (MS) combined with immunoprecipitation to identify the unknown UH-RA.305 antigen. A synovial tissue lysate from the knee of an RA patient will be incubated with the antibody, allowing the antibody to bind to the antigen of interest. Following elution, mass spectrometry of the antigen will be carried out. A protein database search engine will be used to match the acquired peptide sequences against known protein sequences. The antigen identification can be verified by performing additional experiments, such as Western blot or functional assays using the antibody against the identified protein.

Optimizing immuno-affinity purification of anti-UH-RA.318 – In addition, we attempted to optimize the purification of anti-UH-RA.318 using different elution buffers. Elution with 0.1 M glycine-HCl, a low pH elution buffer (pH 2.5), is commonly used for affinity purification (61). To prevent permanent damage to the antibody, the eluted fractions are immediately neutralized using an alkaline buffer such as 1 M

Tris-HCl (pH 9) (61). However, preliminary data indicated that even after neutralization, the anti-UH-RA.318 antibody loses its reactivity, suggesting that the low pH elution damages the antibody (not shown). Therefore, we tested elution conditions involving high ionic strength (3.6M-4.5 M $MgCl_2$, 3.5 M KCl) and high pH (0.1 M glycine-NaOH, pH 10). The high salt concentration in the former disrupts electrostatic interactions, reducing the binding of the antibody to the stationary phase (i.e. immobilized UH-RA.318 peptide on chromatography resin) and facilitating elution (61, 62). In addition to pH and ionic strength conditions, affinity purification is sometimes conducted using denaturants and organic solvents (61). However, due to their harsh nature, we decided to exclude them from the study (61). Interestingly, David A *et al.* and Tsang *et al.* described the optimal dissociation (elution) reagent as $MgCl_2$ with 25% ethylene glycol and $MgCl_2$ with 25% ethylene glycol combined with 0.075 M Hepes/NaOH (pH 7.2), respectively (63, 64). Ethylene glycol acts as a chaotropic agent, meaning it disrupts the hydrogen bonds that stabilizes the antigen-antibody complex (61, 65). However, none of these elution buffers were able to disrupt the interaction between the anti-UH-RA.318 antibody and its corresponding UH-RA.318 peptide.

Interestingly, the ÄKTAprime™ plus purification system can play a significant role in optimizing the purification process for anti-UH-RA.305/318 (56, 59, 66). The ÄKTA chromatography system offers more control over various purification parameters, including flow rates, elution buffers, and sample loading (59, 66). This level of control enables fine-tuning of the purification conditions, which is crucial for optimizing the elution step to achieve the highest antibody recovery and reactivity. Additionally, the ÄKTA system provides automated sample handling capabilities, such as sample loading, column equilibration, and elution (59, 66). This automation reduces manual handling errors and ensures reproducibility, resulting in consistent purification outcomes. Furthermore, ÄKTA supports a range of column types and sizes, allowing for flexibility in selecting the most suitable column for immunoaffinity chromatography (56, 59, 66).

Anti-UH-RA.305 targets specifically the lining of synovial villus tissue surrounding inflammatory infiltrates – Immunohistochemical analysis of the antigenic target tissue expression
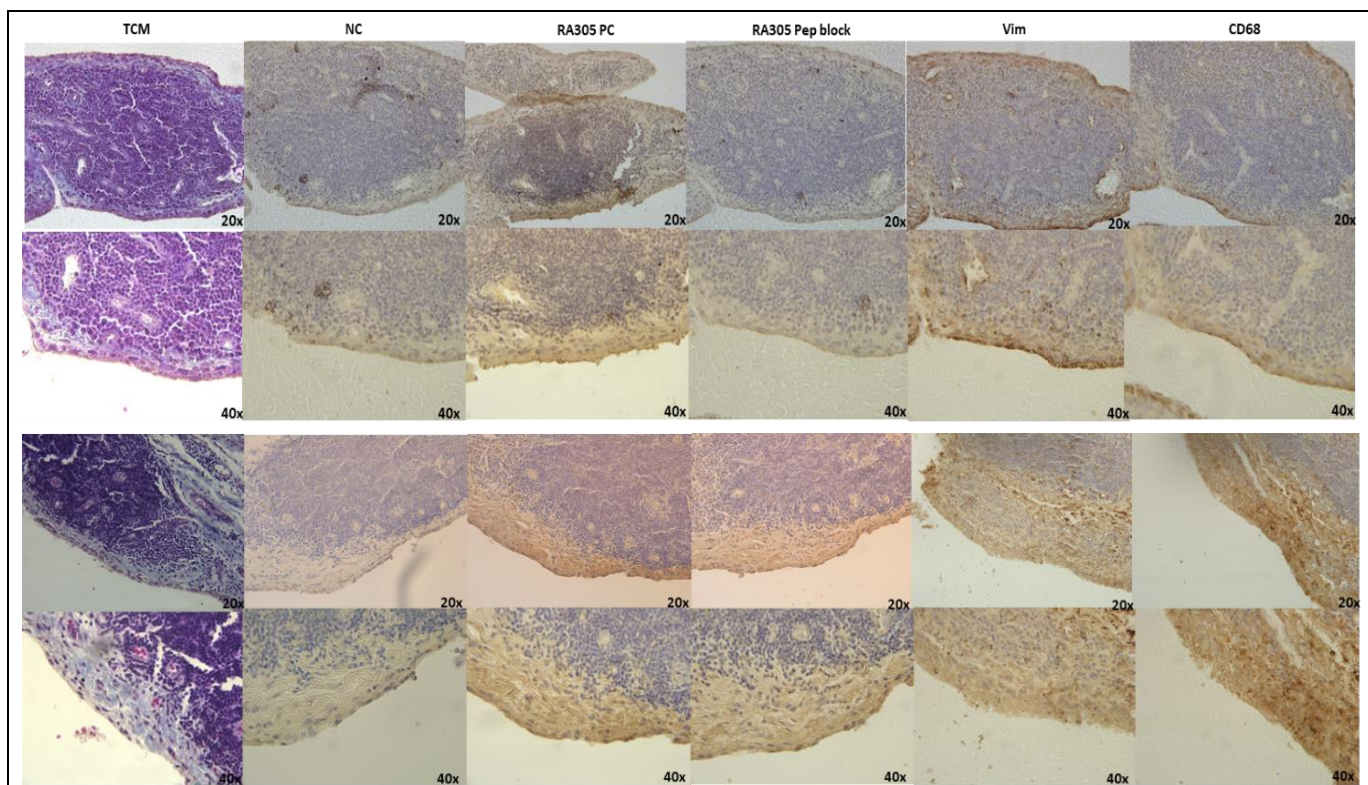
Fig.8 – **The anti-UH-RA.305 antibody specifically targets fibroblasts in the synovial lining** Representative stainings of synovial knee tissue sections from one RA patient. NC, i.e. tissue incubated with 1xPBS, showed no staining. RA305 PC, i.e. tissue incubated with pre-depleted purified anti-UH-RA.305, targets fibroblasts in the lining of synovial villus surrounding inflammatory infiltrates. RA305 pep block, i.e. tissue incubated with anti-UH-RA305 and 4 mg/ml of UH-RA.305 peptide, showed reduced staining in the synovial lining. Vimentin (1/200:1/400 dilution ratio) and CD68 (1/200:1/200 dilution ratio) stains the lining of synovial villus. Staining was performed with DAB (brown) and haematoxylin mayer counterstaining (blue). TCM: Trichroom Masson; NC: Negative Control; PC: Positive Control; Pep: Peptide; Vim: Vimentin; CD68: Cluster of Differentiation 68

of anti-UH-RA.305 revealed its presence in the lining of synovial villus tissue surrounding inflammatory infiltrates (Fig.1, Fig.6&8). The negative control, where only 1xPBS was used, did not show any staining, indicating that the staining observed is not due to non-specific binding of the antibody, or artifacts, but is indeed specific to the synovial lining (Fig.1, Fig.6&8). In addition, 4 mg/ml of UH-RA.305 peptide was used to compete with the anti-UH-RA.305 antibody for binding to the *in vivo* antigen. The peptide block displayed decreased staining, further supporting the antibody specificity. In addition, to validate the specificity of staining, a competition ELISA was conducted. The anti-UH-RA.305 antibody positivity, reflected by the ratio, decreased upon increasing UH-RA.305 peptide concentration (Fig.4A). On the other hand, an irrelevant control peptide did not affect the antibody positivity, thereby reinforcing the validity of the competition ELISA. Accordingly, the competition ELISA and peptide block strengthens the evidence for the specificity of the antibody and confirms that the

observed staining in the synovial lining is indeed attributed to the antibody.

Anti-UH-RA.305 targets fibroblasts in the synovial lining – The synovial membrane is composed of an intimal lining layer that is about 1 to 2 cells thick, as well as a distinct synovial sublining layer (10, 67). The intimal layer comprises fibroblast-like synoviocytes (FLS) , also known as synovial fibroblasts or type B synoviocytes, interspersed with macrophage-like synoviocytes (MLS), also referred to as type A synoviocytes (67). The sublining layer is a well-vascularized connective tissue that contains collagen fibers. Additionally, FLS and MLS are evenly distributed throughout this layer (67). In RA, the intimal lining undergoes hyperplasia, thereby expanding to a thickness of 10 to 20 cells (10, 67, 68). This expansion is primarily attributed to an increase in FLS, but it is driven by the infiltration of bone marrow-derived MLS recruited from the bloodstream (67). The MLS secrete pro-inflammatory cytokines, chemokines and growth factors to the intimal FLS (10).

Subsequently, FLS are induced to proliferate, producing pro-inflammatory cytokines and matrix-degrading molecules, thereby actively perpetuating synovial inflammation (10, 67, 69). To investigate whether the observed anti-UH-RA.305 antibody staining in the synovial lining, corresponds to FLS and/or MLS, it was necessary to optimize immunohistochemistry for relevant markers on these synoviocytes. The type A synovial cells express markers closely related with other macrophage populations, as evidenced by the expression of markers such as CD68 and class II major histocompatibility antigens (10, 70). CD68, is a commonly used marker to identify synovial macrophages in the synovium of RA patients (71, 72). On the other hand, type B synoviocytes display several fibroblast-like characteristics as they express vimentin and different types of collagens (10, 73). Subsequently, optimization of vimentin and CD68 immunohistochemical staining was conducted (Fig.5). Interestingly, after consultation with Prof. dr. Frank Vandenabeele and Prof. dr. Anouk Agten, both pathologists, the anti-UH-RA.305 antibody specifically targets fibroblasts in the lining of synovial villi (Fig.6-8). However, further experiments such as immunofluorescence are warranted in order to confirm colocalization. Furthermore, vimentin is considered a general fibroblast marker, hence an alternative marker that may provide better specificity would be more convenient. Cadherin-11 is one of the major FLS markers and is involved in activating FLS to secrete inflammatory factors including IL-6 contributing to RA (10, 74, 75). In addition, it has been reported that cadherin-11 knockout mice lacks an intimal synovial lining and exhibit reduced cartilage damage induced by RA, highlighting the importance of cadherin-11 (76).

Future perspectives – In the future, we aim to perform *in vitro* functional assays on FLS and osteoclasts to further characterize the biological properties of the antibody. Furthermore, we want to investigate the effect of passive transfer of the anti-UH-RA.305 antibody on the efficacy of first-line therapy response in an animal model for RA. The collagen-induced arthritis (CIA) mouse model is the gold standard to recapitulate RA (77). Following the onset of symptoms, the CIA mice will be treated with MTX and anti-UH-RA.305 antibody. Clinical signs of ankle joint swelling and inflammation will be measured using a semi-quantitative scoring system (78). Lastly, after sacrificing the mice, the joint inflammation, cartilage destruction and bone loss will be evaluated to determine the pathological role of anti-UH-RA.305.

CONCLUSION

In conclusion, we have optimized the purification of anti-UH-RA.305 and identified its antigenic tissue localization. Anti-UH-RA.305 has been shown to specifically target the lining of synovial villus tissue surrounding inflammatory infiltrates. The staining specificity was validated by a UH-RA.305 peptide block and competition ELISA. Moreover, immunohistochemical staining was optimized for two leading cell types in the synovial lining, fibroblast-like synoviocytes and macrophage-like synoviocytes. Subsequently, the anti-UH-RA.305 antibody was demonstrated to target fibroblasts in the lining of synovial villi. In the future, we aim at further biological characterization of anti-UH-RA.305, through immunofluorescence (colocalization), *in vitro* functional assays and *in vivo* animal experiments. This will lead to a better understanding of the role of anti-UH-RA.305 in RA pathogenesis and potentially identify novel therapeutic targets. Accordingly, this could significantly improve the management of RA for the one-third of patients who currently experience prolonged disease activity due to a lack of response to first-line treatments.

REFERENCES

1.   Organization WH. Musculoskeletal health 14 July 2022 [Available from: https://www.who.int/news-room/fact-sheets/detail/musculoskeletal-conditions.

2.   Gerosa M, De Angelis V, Riboldi P, Meroni PL. Rheumatoid arthritis: a female challenge. Womens Health (Lond). 2008;4(2):195-201.

3.   Shams S, Martinez JM, Dawson JRD, Flores J, Gabriel M, Garcia G, et al. The Therapeutic Landscape of Rheumatoid Arthritis: Current State and Future Directions. Frontiers in Pharmacology. 2021;12.

4.   Vandormael P, Verschueren P, De Winter L, Somers V. cDNA phage display for the discovery of theranostic autoantibodies in rheumatoid arthritis. Immunol Res. 2017;65(1):307-25.

5.   van den Hoek J, Roorda LD, Boshuizen HC, Tijhuis GJ, van den Bos GA, Dekker J. Physical and Mental Functioning in Patients with Established Rheumatoid Arthritis over an 11-year Followup Period: The Role of Specific Comorbidities. The Journal of Rheumatology. 2016;43(2):307-14.

6.   Nurmohamed MT, Heslinga M, Kitas GD. Cardiovascular comorbidity in rheumatic diseases. Nature Reviews Rheumatology. 2015;11(12):693-704.

7.   De Winter LM, Hansen WL, van Steenbergen HW, Geusens P, Lenaerts J, Somers K, et al. Autoantibodies to two novel peptides in seronegative and early rheumatoid arthritis. Rheumatology (Oxford). 2016;55(8):1431-6.

8.   Gioia C, Lucchino B, Tarsitano MG, Iannuccelli C, Di Franco M. Dietary Habits and Nutrition in Rheumatoid Arthritis: Can Diet Influence Disease Development and Clinical Manifestations? Nutrients. 2020;12(5).

9.   Gabriel SE. Why do people with rheumatoid arthritis still die prematurely? Ann Rheum Dis. 2008;67 Suppl 3(Suppl 3):iii30-4.

10.   Bartok B, Firestein GS. Fibroblast-like synoviocytes: key effector cells in rheumatoid arthritis. Immunological Reviews. 2010;233(1):233-55.

11.   Firestein GS. Invasive fibroblast-like synoviocytes in rheumatoid arthritis. Passive responders or transformed aggressors? Arthritis Rheum. 1996;39(11):1781-90.

12.   Sweeney SE, Firestein GS. Rheumatoid arthritis: regulation of synovial inflammation. Int J Biochem Cell Biol. 2004;36(3):372-8.

13.   Smolen JS, Landewé RBM, Bijlsma JWJ, Burmester GR, Dougados M, Kerschbaumer A, et al. EULAR recommendations for the management of rheumatoid arthritis with synthetic and biological disease-modifying antirheumatic drugs: 2019 update. Ann Rheum Dis. 2020;79(6):685-99.

14.   Westhovens R, Verschueren P. Defining remission in patients with RA in clinical practice. Nature Reviews Rheumatology. 2012;8(8):445-7.

15.   Friedman B, Cronstein B. Methotrexate mechanism in treatment of rheumatoid arthritis. Joint Bone Spine. 2019;86(3):301-7.

16.   Cronstein BN, Eberle MA, Gruber HE, Levin RI. Methotrexate inhibits neutrophil function by stimulating adenosine release from connective tissue cells. Proc Natl Acad Sci U S A. 1991;88(6):2441-5.

17.   Cronstein BN, Levin RI, Belanoff J, Weissmann G, Hirschhorn R. Adenosine: an endogenous inhibitor of neutrophil-mediated injury to endothelial cells. J Clin Invest. 1986;78(3):760-70.

18.   Maciejewski M, Sands C, Nair N, Ling S, Verstappen S, Hyrich K, et al. Prediction of response of methotrexate in patients with rheumatoid arthritis using serum lipidomics. Sci Rep. 2021;11(1):7266.

19.   De Cock D, Vanderschueren G, Meyfroidt S, Joly J, Van der Elst K, Westhovens R, et al. The performance of matrices in daily clinical practice to predict rapid radiologic progression in patients with early RA. Seminars in Arthritis and Rheumatism. 2014;43(5):627-31.

20.   Wu CY, Yang HY, Luo SF, Lai JH. From Rheumatoid Factor to Anti-Citrullinated Protein Antibodies and Anti-Carbamylated Protein Antibodies for Diagnosis and Prognosis Prediction in Patients with Rheumatoid Arthritis. Int J Mol Sci. 2021;22(2).

21.   Smolen JS, Aletaha D, Barton A, Burmester GR, Emery P, Firestein GS, et al. Rheumatoid arthritis. Nat Rev Dis Primers. 2018;4:18001.

22.   Lin YJ, Anzaghe M, Schülke S. Update on the Pathomechanism, Diagnosis, and Treatment Options for Rheumatoid Arthritis. Cells. 2020;9(4).

23.   van Delft MAM, Huizinga TWJ. An overview of autoantibodies in rheumatoid arthritis. J Autoimmun. 2020;110:102392.

24.   Möttönen T, Paimela L, Leirisalo-Repo M, Kautiainen H, Ilonen J, Hannonen P. Only high disease activity and positive rheumatoid factor indicate poor prognosis in patients with early rheumatoid arthritis treated with "sawtooth" strategy. Ann Rheum Dis. 1998;57(9):533-9.

25.   Bukhari M, Lunt M, Harrison BJ, Scott DG, Symmons DP, Silman AJ. Rheumatoid factor is the major predictor of increasing severity of radiographic erosions in rheumatoid arthritis: results from the Norfolk Arthritis Register Study, a large inception cohort. Arthritis Rheum. 2002;46(4):906-12.

26.   Rönnelid J, Wick MC, Lampa J, Lindblad S, Nordmark B, Klareskog L, et al. Longitudinal analysis of citrullinated protein/peptide antibodies (anti-CP) during 5 year follow up in early rheumatoid arthritis: anti-CP status predicts worse disease activity and greater radiological progression. Ann Rheum Dis. 2005;64(12):1744-9.

27.   van der Helm-van Mil AH, Verpoort KN, Breedveld FC, Toes RE, Huizinga TW. Antibodies to citrullinated proteins and differences in clinical progression of rheumatoid arthritis. Arthritis Res Ther. 2005;7(5):R949-58.

28.   Nielen MMJ, van Schaardenburg D, Reesink HW, van de Stadt RJ, van der Horst-Bruinsma IE, de Koning MHMT, et al. Specific autoantibodies precede the symptoms of rheumatoid arthritis: A study of serial measurements in blood donors. Arthritis & Rheumatism. 2004;50(2):380-6.

29.   de Brito Rocha S, Baldo DC, Andrade LEC. Clinical and pathophysiologic relevance of autoantibodies in rheumatoid arthritis. Advances in Rheumatology. 2019;59(1):2.

30.   Uysal H, Bockermann R, Nandakumar KS, Sehnert B, Bajtner E, Engström A, et al. Structure and pathogenicity of antibodies specific for citrullinated collagen type II in experimental arthritis. J Exp Med. 2009;206(2):449-62.

31.   Falkenburg WJJ, von Richthofen HJ, Rispens T. On the origin of rheumatoid factors: Insights from analyses of variable region sequences. Semin Arthritis Rheum. 2019;48(4):603-10.

32.   Meta-analysis: Diagnostic Accuracy of Anti–Cyclic Citrullinated Peptide Antibody and Rheumatoid Factor for Rheumatoid Arthritis. Annals of Internal Medicine. 2007;146(11):797-808.

33.   Sokolove J, Zhao X, Chandra PE, Robinson WH. Immune complexes containing citrullinated fibrinogen costimulate macrophages via Toll-like receptor 4 and Fcγ receptor. Arthritis Rheum. 2011;63(1):53-62.

34.   Laurent L, Anquetil F, Clavel C, Ndongo-Thiam N, Offer G, Miossec P, et al. IgM rheumatoid factor amplifies the inflammatory response of macrophages induced by the rheumatoid arthritis-specific immune complexes containing anticitrullinated protein antibodies. Ann Rheum Dis. 2015;74(7):1425-31.

35.   Kuhn KA, Kulik L, Tomooka B, Braschler KJ, Arend WP, Robinson WH, et al. Antibodies against citrullinated proteins enhance tissue injury in experimental autoimmune arthritis. J Clin Invest. 2006;116(4):961-73.

36.   Harre U, Georgess D, Bang H, Bozec A, Axmann R, Ossipova E, et al. Induction of osteoclastogenesis and bone loss by human autoantibodies against citrullinated vimentin. J Clin Invest. 2012;122(5):1791-802.

37.   Wigerblad G, Bas DB, Fernades-Cerqueira C, Krishnamurthy A, Nandakumar KS, Rogoz K, et al. Autoantibodies to citrullinated proteins induce joint pain independent of inflammation via a chemokine-dependent mechanism. Ann Rheum Dis. 2016;75(4):730-8.

38.   Sellam J, Hendel-Chavez H, Rouanet S, Abbed K, Combe B, Le Loët X, et al. B cell activation biomarkers as predictive factors for the response to rituximab in rheumatoid arthritis: A six-month, national, multicenter, open-label study. Arthritis & Rheumatism. 2011;63(4):933-8.

39.   Isaacs JD, Cohen SB, Emery P, Tak PP, Wang J, Lei G, et al. Effect of baseline rheumatoid factor and anticitrullinated peptide antibody serotype on rituximab clinical response: a meta-analysis. Annals of the Rheumatic Diseases. 2013;72(3):329-36.

40.   Chatzidionysiou K, Lie E, Nasonov E, Lukina G, Hetland ML, Tarp U, et al. Highest clinical effectiveness of rituximab in autoantibody-positive patients with rheumatoid arthritis and in those for whom no more than one previous TNF antagonist has failed: pooled data from 10 European registries. Annals of the Rheumatic Diseases. 2011;70(9):1575-80.

41.   Lal P, Su Z, Holweg CT, Silverman GJ, Schwartzman S, Kelman A, et al. Inflammation and autoantibody markers identify rheumatoid arthritis patients with enhanced clinical benefit following rituximab treatment. Arthritis Rheum. 2011;63(12):3681-91.

42.   Lv Q, Yin Y, Li X, Shan G, Wu X, Liang D, et al. The status of rheumatoid factor and anti-cyclic citrullinated peptide antibody are not associated with the effect of anti-TNFα agent treatment in patients with rheumatoid arthritis: a meta-analysis. PLoS One. 2014;9(2):e89442.

43.   Hider SL, Silman AJ, Thomson W, Lunt M, Bunn D, Symmons DP. Can clinical factors at presentation be used to predict outcome of treatment with methotrexate in patients with early inflammatory polyarthritis? Ann Rheum Dis. 2009;68(1):57-62.

44.   Drouin J, Haraoui B. Predictors of clinical response and radiographic progression in patients with rheumatoid arthritis treated with methotrexate monotherapy. J Rheumatol. 2010;37(7):1405-10.

45.   Saevarsdottir S, Wallin H, Seddighzadeh M, Ernestam S, Geborek P, Petersson IF, et al. Predictors of response to methotrexate in early DMARD naive rheumatoid arthritis: results from the initial open-label phase of the SWEFOT trial. Ann Rheum Dis. 2011;70(3):469-75.

46.   Hoekstra M, van Ede AE, Haagsma CJ, van de Laar MA, Huizinga TW, Kruijsen MW, et al. Factors associated with toxicity, final dose, and efficacy of methotrexate in patients with rheumatoid arthritis. Ann Rheum Dis. 2003;62(5):423-6.

47.   Wessels JA, van der Kooij SM, le Cessie S, Kievit W, Barerra P, Allaart CF, et al. A clinical pharmacogenetic model to predict the efficacy of methotrexate monotherapy in recent-onset rheumatoid arthritis. Arthritis Rheum. 2007;56(6):1765-75.

48.   Gossec L, Dougados M, Goupille P, Cantagrel A, Sibilia J, Meyer O, et al. Prognostic factors for remission in early rheumatoid arthritis: a multiparameter prospective study. Ann Rheum Dis. 2004;63(6):675-80.

49.   Verstappen SM, van Albada-Kuipers GA, Bijlsma JW, Blaauw AA, Schenk Y, Haanen HC, et al. A good response to early DMARD treatment of patients with rheumatoid arthritis in the first year predicts remission during follow up. Ann Rheum Dis. 2005;64(1):38-43.

50.   Forslind K, Ahlmén M, Eberhardt K, Hafström I, Svensson B. Prediction of radiological outcome in early rheumatoid arthritis in clinical practice: role of antibodies to citrullinated peptides (anti-CCP). Ann Rheum Dis. 2004;63(9):1090-5.

51.   Kastbom A, Strandberg G, Lindroos A, Skogh T. Anti-CCP antibody test predicts the disease course during 3 years in early rheumatoid arthritis (the Swedish TIRA project). Ann Rheum Dis. 2004;63(9):1085-9.

52.   Ponchel F, Goëb V, Parmar R, El-Sherbiny Y, Boissinot M, El Jawhari J, et al. An immunological biomarker to predict MTX response in early RA. Ann Rheum Dis. 2014;73(11):2047-53.

53.   Peres RS, Liew FY, Talbot J, Carregaro V, Oliveira RD, Almeida SL, et al. Low expression of CD39 on regulatory T cells as a biomarker for resistance to methotrexate therapy in rheumatoid arthritis. Proc Natl Acad Sci U S A. 2015;112(8):2509-14.

54.   Vandormael P, Pues A, Sleurs E, Liesenborgs J, Verschueren P, Somers V. POS0144 NOVEL ANTIBODY BIOMARKERS THAT PREDICT FAILURE TO ACHIEVE EARLY AND SUSTAINED DISEASE REMISSION OR LOW DISEASE ACTIVITY AFTER INTENSIVE FIRST-LINE THERAPY IN RHEUMATOID ARTHRITIS. Annals of the Rheumatic Diseases. 2022;81:299.1-.

55.   Stouten V, Westhovens R, Pazmino S, De Cock D, Van der Elst K, Joly J, et al. Effectiveness of different combinations of DMARDs and glucocorticoid bridging in early rheumatoid arthritis: two-year results of CareRA. Rheumatology (Oxford). 2019;58(12):2284-94.

56.   Sciences GHL. Prepacked chromatography columns for ÄKTA systems [Available from: https://us.vwr.com/assetsvc/asset/en_US/id/13683616/contents.

57.   Scheffel J, Hober S. Highly selective Protein A resin allows for mild sodium chloride-mediated elution of antibodies. Journal of Chromatography A. 2021;1637:461843.

58.   Rispens T, Vidarsson G. Chapter 9 - Human IgG Subclasses. In: Ackerman ME, Nimmerjahn F, editors. Antibody Fc. Boston: Academic Press; 2014. p. 159-77.

59.   Sciences GHL. ÄKTA Laboratory-scale Chromatography Systems [Available from: https://www2.fcfar.unesp.br/Home/Instituicao/Departamentos/cienciasbiologicasnovo/laboratoriomultiusuariosfinep/akta_instrument_management.pdf.

60. Brechmann NA, Eriksson PO, Eriksson K, Oscarsson S, Buijs J, Shokri A, et al. Pilot-scale process for magnetic bead purification of antibodies directly from non-clarified CHO cell culture. Biotechnol Prog. 2019;35(3):e2775.

61. Scientific T. Optimize elution conditions for immunoaffinity purification [Available from: https://assets.thermofisher.com/TFS-Assets/LSG/Application-Notes/TR0027-Elution-conditions.pdf.

62. Sigma-Aldrich. Practical Considerations for IEX Separation [Available from: https://www.sigmaaldrich.com/BE/en/technical-documents/technical-article/protein-biology/protein-purification/iex-separation.

63. Ben-David A, Firer MA. Immunoaffinity purification of monoclonal antibodies: In search of an elution buffer of general applicability. Biotechnology Techniques. 1996;10(10):799-802.

64. Tsang VC, Wilkins PP. Optimum dissociating condition for immunoaffinity and preferential isolation of antibodies with high specific activity. J Immunol Methods. 1991;138(2):291-9.

65. Vuksanović JM, Kijevčanin ML, Radović IR. Poly(ethylene glycol) diacrylate as a novel chaotropic compound for design of aqueous biphasic systems. Journal of Molecular Liquids. 2018;261:250-64.

66. Sciences GHL. ÄKTAprime plus Operating Instructions [Available from: https://cdn.cytivalifesciences.com/api/public/content/digi-14489-original.

67. Ouboussad L, Burska AN, Melville A, Buch MH. Synovial Tissue Heterogeneity in Rheumatoid Arthritis and Changes With Biologic and Targeted Synthetic Therapies to Inform Stratified Therapy. Frontiers in Medicine. 2019;6.

68. Firestein GS. PATHOGENESIS OF RHEUMATOID ARTHRITIS: THE INTERSECTION OF GENETICS AND EPIGENETICS. Trans Am Clin Climatol Assoc. 2018;129:171-82.

69. Müller-Ladner U, Ospelt C, Gay S, Distler O, Pap T. Cells of the synovium in rheumatoid arthritis. Synovial fibroblasts. Arthritis Research & Therapy. 2007;9(6):223.

70. Asif Amin M, Fox DA, Ruth JH. Synovial cellular and molecular markers in rheumatoid arthritis. Semin Immunopathol. 2017;39(4):385-93.

71. Tak PP, Smeets TJ, Daha MR, Kluin PM, Meijers KA, Brand R, et al. Analysis of the synovial cell infiltrate in early rheumatoid synovial tissue in relation to local disease activity. Arthritis Rheum. 1997;40(2):217-25.

72. Mulherin D, Fitzgerald O, Bresnihan B. Synovial tissue macrophage populations and articular damage in rheumatoid arthritis. Arthritis Rheum. 1996;39(1):115-24.

73. Tu J, Hong W, Zhang P, Wang X, Körner H, Wei W. Ontology and Function of Fibroblast-Like and Macrophage-Like Synoviocytes: How Do They Talk to Each Other and Can They Be Targeted for Rheumatoid Arthritis Therapy? Front Immunol. 2018;9:1467.

74. Yoshitomi H. Regulation of Immune Responses and Chronic Inflammation by Fibroblast-Like Synoviocytes. Frontiers in Immunology. 2019;10.

75. Chang SK, Noss EH, Chen M, Gu Z, Townsend K, Grenha R, et al. Cadherin-11 regulates fibroblast inflammation. Proceedings of the National Academy of Sciences. 2011;108(20):8402-7.

76. Lee DM, Kiener HP, Agarwal SK, Noss EH, Watts GF, Chisaka O, et al. Cadherin-11 in synovial lining formation and pathology in arthritis. Science. 2007;315(5814):1006-10.

77. Brand DD, Latham KA, Rosloniec EF. Collagen-induced arthritis. Nat Protoc. 2007;2(5):1269-75.

78. Seeuws S, Jacques P, Van Praet J, Drennan M, Coudenys J, Decruy T, et al. A multiparameter approach to monitor disease activity in collagen-induced arthritis. Arthritis Res Ther. 2010;12(4):R160.